Atmos. Chem. Phys. Discuss., 7, 15067–15103, 2007
www.atmos-chem-phys-discuss.net/7/15067/2007/
© Author(s) 2007. This work is licensed
under a Creative Commons License.

Atmospheric Chemistry and Physics Discussions

NO_2 climatology in the northern subtropical region: diurnal, seasonal and interannual variability

M. Gil[1], M. Yela[1], L. N. Gunn[2], A. Richter[3], I. Alonso[1], M. P. Chipperfield[2], E. Cuevas[4], J. Iglesias[1], M. Navarro[1], O. Puentedura[1], and S. Rodríguez[1]

[1]Area de Investigación e Instrumentación Atmosférica, INTA, Torrejón de Ardoz, Spain
[2]Inst. for Atmospheric Science, School of Earth and Environment, Univ. of Leeds, Leeds, UK
[3]Institute of Environmental Physics, University of Bremen, Bremen, Germany
[4]Centro de Investigación Atmosférica de Izaña, INM, Sta. Cruz de Tenerife, Spain

Received: 2 October 2007 – Accepted: 10 October 2007 – Published: 19 October 2007

Correspondence to: M. Gil (gilm@inta.es)

Abstract

Daily NO_2 vertical column density (VCD) has been routinely measured by zenith sky spectroscopy at the subtropical station of Izaña (28° N, 16° W) since 1993 in the framework of the Network for the Detection of Atmospheric Composition Change (NDACC). Based on 14 years of data the first low latitudes NO_2 VCD climatology has been established and the main characteristics from short scales of one day to inter-annual variability are presented. Instrumental descriptions and different source of errors are described in detail. The observed diurnal cycle follows that expected by gas-phase NOx chemistry, as can be shown by the good agreement with a vertically integrated chemical box model, and is modulated by solar radiation. The seasonal evolution departs from the phase of the hours of daylight, showing the signature of upper stratospheric temperature changes. From the data record no significant long-term trends in NO_2 VCD can be inferred. Comparison of the ground-based data sets with nadir looking satellite spectrometers shows excellent agreement for SCIAMACHY with differences between both datasets of 1.1%. GOME displays unrealistic features with largest discrepancies during summer. The ground-based data are compared with long-term output of the SLIMCAT 3-D chemical transport model (CTM). The basic model, forced by ECMWF (ERA-40) analyses, captures the observed NO_2 annual cycle but significantly underestimates the spring/summer maximum. In a model run which uses assimilation of satellite CH_4 profiles to constrain the model long-lived tracers the agreement is significantly improved. This improvement in modelled column NO_2 is due to better modelled NOy profiles and points to transport errors in the ECMWF ERA-40 reanalyses.

1 Introduction

NO_2 plays an important role in the chemistry of ozone from the mid stratosphere to the mesosphere through catalytic reactions:

$$NO + O_3 \rightarrow NO_2 + O_2 \quad (1)$$

ACPD
7, 15067–15103, 2007

$$NO_2 + O \rightarrow NO + O_2 \quad (2)$$

$$\text{Net} : O_3 + O \rightarrow 2O_2 \quad (3)$$

Contribution to the overall O_3 equilibrium depends on latitude, height and season. The primary source of stratospheric active nitrogen is from N_2O (Minschwaner et al., 1993). In the mid and upper stratosphere N_2O is converted to NO by reaction with excited oxygen atoms $O(^1D)$ produced mainly by UV photolysis of O_3. Recent measurements have shown a steady increase in the N_2O atmospheric concentration over the last two decades of 2.2–2.6% per decade (WMO 2007). While the chemistry of the NOy family has been well established over the last decades, NO_2 long term observations display positive trends exceeding that of N_2O. Liley et al. (2000) find increases of 5±1% when analyzing the longest data set available using visible spectroscopy (Lauder, New Zealand), for the 1980–1999 period, some 2% larger than the estimated trend in N_2O. The same rate of increase (+5.2±3.2% per decade) is obtained by Rinsland et al. (2003) for Kitt Peak (32° N) by a FTIR spectrometer. Struthers et al. (2004) compared two southern hemisphere data sets at mid (Lauder, New Zealand 45° S) and polar-latitudes (Arrival Height, Antarctica, 78° S) and with a chemistry-climatic model (CCM) again, finding an underestimation in the trend obtained by the model in more than 2% per decade for the period 1980–2000.

Differential optical absorption spectrometry (DOAS) in the visible range has been extensively used for ground-based NO_2 vertical column density (VCD) measurements since the pioneering work of Brewer (1973) and Noxon (1975) and further improvements by Solomon et al. (1987) and others.

Since the late 1980s and 1990s zenith spectrometers have been deployed at remote locations around the globe for NO_2 stratospheric studies. Most of them are integrated in the Network for Detection of Atmospheric Composition Change (NDACC), formerly NDSC, following a measurement protocol and participating in regular intercomparisons for quality assurance (see NDACC web page). These data have helped establish a better understanding of nitrogen oxides stratospheric behaviour in the extra-tropical

ACPD
7, 15067–15103, 2007

EGU

region. In 1993 Izaña (28° N) initiated its routine measurements program for NO_2, later extended to O_3 and BrO. Also in the early nineties four stations were set up in the frame of the SAOZ network in the southern hemisphere (see SAOZ web page). Recently, two more were added to the BREDOM network (Medeke et al., 2005). However, long records in the tropical latitude belt are still scarce and no comprehensive long-term low latitude NO_2 measurements have been reported to date.

In the last decade, the technique has been successfully extended to satellites instruments such as GOME, SCIAMACHY and OMI and will continue in the years to come with the GOME-2, a set of units on board of the operational METOP series. While polar orbiting satellites offer the advantage of global coverage, no diurnal variation study is possible since they scan once per day at best the low latitudes region. Additionally, orbiting instruments require validation from the ground to establish the optimum settings and detect potential degradation with time. Quality controlled instrumentation provide independent measurement stable in time useful in extreme for orbiting instrument checking.

The UV-Vis spectrometer network has contributed to the NO_2 validation processing of satellite instruments such as GOME (Lambert et al., 1998, Richter et al., 2000) on board of the ERS-2 and extensively to SCIAMACHY (Lambert et al., 2004, Richter et al., 2004, Piters et al., 2006, Lambert et al., 2007 and others) and MIPAS (Hendrick et al., 2004, Wetzel et al., 2007) on the ENVISAT platform.

We report here the behaviour of the NO_2 column over Izaña, an unpolluted site located in the northern subtropics (28° N, 16° W), based on 14 years of data from diurnal to interannual scales. Ground-based observational data are compared to models and satellite measurements for the location, constituting a limited low-latitude NO_2 climatology for the recorded period.

2 Passive DOAS at zenith

The technique used is based on measurement of atmospheric absorption of solar radiation in selected wavelength bands where NO_2 has a structured cross-section. For stratospheric observations the instrument is pointed to the zenith sky. Under these conditions, the equivalent path for a given wavelength is defined as the single path that behaves to the observed absorption as the sum of all paths contributing to the zenith radiation weighted by the intensity of each one. At twilight, the equivalent path is dominated by the stratospheric contribution since the slant path is enhanced compared to the tropospheric one.

The logarithm of this equivalent twilight spectrum, ideally ratioed to an extraterrestrial spectrum, yields the optical depth of the absorbants, providing the Lambert-Beer equation applies which is the case in an optically thin atmosphere. In practice, the extraterrestrial spectrum is substituted by a spectrum measured at high sun. The measured slant column NO_2 density (SCD) is in fact the difference between two slant paths, a so called Differencial Slant Column Density (DSCD).

The DOAS at zenith technique requires that all absorbers and scatterers are known in advance and that their absorption cross-sections are known in the spectral range selected. When solving the Lambert-Beer equation care must be taken to precisely align the reference and measured spectra. For that purpose spectral stretch and shift are included as non-linear parameters yielding the following equation:

$$(d/dN_i)\{\ln^* \left[\frac{I(a\lambda + b)}{I_0(c\lambda + d)}\right] = +\Sigma\{\sigma_i^*(\lambda).N_i\}\}^2 = \varepsilon(\text{minimum}) \quad (4)$$

Where a, c and b, d are respectively squeeze and shift of the twilight spectrum I, and of the high sun spectrum, I_0. N_i are the slant densities of the absorbers and scatterers, and * denotes the orthogonalised natural logarithm and cross-sections.

To convert the spectral observations to vertical column density (VCD) a further two step process is required. First the amount of the NO_2 density contained in the reference

ACPD
7, 15067–15103, 2007

EGU

spectrum must be computed and added to the DSCD, and then the vertical column conversion is performed by dividing with the Air Mass Factor (AMF) coefficients.

2.1 Reference content and AMF calculations

The amount of gas contained in the reference spectrum in species dynamically controlled as for O_3 can be obtained as the intercept in a linear fit by the classical Langley plot method:

$$\text{Ref} = \text{VCD} * \text{AMF(sza)} - \text{SCD(sza)} \quad (5)$$

where, VCD is the vertical column density of O_3, and SCD(sza) is the retrieved amount from the observations. AMF(sza) are mainly a function of solar zenith angle (sza) but dependent to some extent on the shape of the vertical profile of the gas under consideration. Ref is the amount contained in the zenith reference spectrum at high sun. It can be retrieved as the intercept of the linear fit under the assumption of no concentration changes during the period of the measurements. Other species of short photochemical lifetime, as is the case with NO_2, suffer significant changes throughout the day, the constant column assumption is not valid and consequently the representation of AMF versus slant column departs from a straight line.

For these species the so-called modified AMF must be used instead (Lee et al., 1994). These AMFs are obtained by including a coefficient C(sza) = VCD_0/VCD(sza) where VCD(sza) comes from a photochemical box model for the season. VCD_0 is the vertical column at the sza where the reference spectrum has been recorded. The correction assumes that the actual NO_2 diurnal variation is proportional to the NO_2 predicted by the model. Then the reference content can be estimated by:

$$\text{Ref} = \text{VCD} * \text{AMF(sza)}.\text{C(sza)} - \text{SCD(sza)} \quad (6)$$

The reference spectrum can be used for many years if the spectrograph does not change its specifications, and the Langley plot is computed only once per reference.

ACPD
7, 15067–15103, 2007

3 The station

The Global Atmospheric Watch (GAW) Izaña station, managed by the Instituto Nacional de Meteorología (INM, Spain) is located at 28° 18′ N, 16° 29′ W on Tenerife (Canary Islands), 300 km from the African west coast at an altitude of 2370 m a.s.l. The Canary Islands are below the descending branch of the Hadley which favours a large scale high stability catabatic flow regime, resulting in a large number of clear-sky days. The appearance of deep lows and cut-off lows, which could favour the stratosphere-troposphere exchange, is constraint to winter time. The station is above a quasi-permanent trade wind inversion well established between 800 and 1500 m a.s.l., only absent during some episodes in winter. As a consequence, the station is under free-troposphere conditions most of the time, precluding pollution from the Sta. Cruz and Puerto de la Cruz coastal towns. In-situ NO_2 annual mean during twiligh are of 115 and 473 pptv for am and pm, respectively (Y. Gonzalez, personal communication). The summer-autumn stratospheric circulation is essentially zonal. Air-masses originate at 20–25° N with little latitudinal variation (Schneider et al., 2005). During winter there is a large variation in the origin of the air masses arriving at the station due to planetary wave activity. Occasionally polar stratospheric air-masses reach the station (Yela, 1999).

3.1 Instrumentation

Two instruments contribute to the data record. In May 1993 a scanning spectrometer was installed on the terrace of the observatory. It is based on a Jobin-Yvon H20 monochromator with a ruled grating of 1200 grooves/mm and a photomultiplier tube Hammamatsu R212-UH blue enhanced as detector. Spectral resolution is 1 nm FWHM and the sampling path is 0.1 nm in the range 430–450 nm. A full spectrum is taken in 1.7 s. and 30 spectra per measurement are accumulated to improve the signal to noise ratio. The instrument is located outdoors in a thermostatised housing. Light reaches the spectrograph by a 45° angle mirror. The instrument takes one measurement per

0.5° of sza between 88° and 92°.

In December 1998 an advanced visible spectrograph was installed. The instrument is based on an EGG&1453A 1024 PDA detector controlled by an EGG 1461 on a Jarrel-Ash Monospec 18 spectrograph with 18 cm focal length. Scattered light at zenith is collected by a baffled cylinder through a quartz fibre bundle with the inner end rectangle-shaped acting as 100 μm entrance slit. A flat ruled diffraction grating of 600 grooves/mm provides a spectral range of 340–600 nm for NO_2 and O_3 observations with an average FWHM resolution of 1.3 nm and an oversampling factor of 5. The spectrograph and detector are housed in a thermostatised hermetic container keeping the spectrograph at a constant temperature of 15±0.2^{o}C, thus maintaining the alignment of the spectra with time. The detector is operated at −35°C by means of a 2-step peltier and external assistance of a circulating chiller at −10°C. A continuous supply of dry nitrogen from a generator prevents ice formation on the detector window. In-house control software keeps the assembly in operation. Measurements are carried out in continuous mode from 94° sza at dawn to 94° at sunset skipping the central hours of the day whenever the sza is smaller than 45° to avoid spectra perturbations due to reflections in the entrance baffle and direct sun. Typical daytime integration time in clear sky is 2.5 s, increasing to 25 s at 90°sza. The instrument is programmed to integrate spectra during the time required for the sun to move 0.2°, therefore about 500 spectra are collected everyday. Midnight spectra are recorded everyday for dark current checking. Spectral resolution is measured periodically by monitoring a low-pressure Hg lamp and whenever an increase in the errors is observed.

Short-term studies and diurnal evolution are carried out with a third instrument. The INTA-ARTIST spectrometer is optimized for BrO measurements covering the 325–460 range at 0.6 nm resolution FWHM. The detector is a Princeton PDA1024 operating at −40°C controlled by a ST121 unit. Light reception is essentially identical to INTA-RASAS except for a narrower FOV. Lower detector noise and high instrumental stability result in a signal to noise 2 times better than the RASAS instrument. The entrance FOV's (half angle) are 8.5°, 6.5°, and 3.2° for EVA, RASAS, and ARTIST, respectively.

ACPD
7, 15067–15103, 2007

EGU

The UV-Vis spectrometer INTA-RASAS has been operating on a routine basis since late 1998 and INTA-ARTIST since 2001. Both are NDACC (formerly NDSC) -qualified instruments. INTA has participated in the OHP 1996 (Roscoe et al., 1999) and Andoya 2003 (Vandaele et al., 2005) NDACC intercomparison exercises.

3.2 Data and settings

Fourteen years of data have been used in the analysis. Due to a refurbishment of the Izaña observatory from 1998 to 2003 the spectrometers were installed in a container separated from the main building. From time to time they suffered failures due to power supply interruptions and high dust produced by the surrounding working machines that reached the spectrograph through the nitrogen generator. In October 2003 the spectrometers were moved again to the upper floor of the main building tower significantly improving the laboratory temperature control and power, resulting in almost no gaps in the data since that date.

NO_2 from the scanning EVA spectrometer is retrieved in the 433–448.5 nm range. The operational RASAS analysis makes use of a large spectral interval (435–540 nm) for simultaneous retrieval of NO_2 and O_3 columns. NO_2 from the ARTIST is evaluated in the 425–450 nm range. The NO_2 absorption cross-sections in this region are highly structured, Gaussian in shape, with a large number of optically active transitions with irregular fine structure superimposed, due to the strong coupling between the ground and first excited electronic states (Orphal, 2002). Doppler broadening, due to thermal motion of the molecules, and pressure broadening are irrelevant for the retrieval at the spectral resolution used in our instruments.

In order to homogenise the results, cross sections used are those defined as standard in the Andoya NDACC (NDSC) intercomparison (Vandaele et al., 2005). A set of 6 cross-sections have been included in the analysis; O_3 at 223 K (Bogumil et al., 2001), NO_2 at 220 K (Vandaele et al., 1998), H_2O from Hitran database (2000) and O_4 at room temperature by Greenblatt et al. (1990). The Raman scattering cross-section was generated by the Windoas package (Fayt and van Roozendael, 2001) from the Raman

theory. Finally a pseudo-cross-section was included to account for stray light inside the spectrograph. Figure 1 shows an example of clear sky fitting results at twilight for all three instruments. The ARTIST performance yields very low residuals (2–3×10^{-4} DOD) while EVA and RASAS are at a similar level (5–6×10^{-4} DOD).

Air Mass Factors were computed by the INTA single scattering radiative transfer model (Sarkissian et al., 1995a) at 440 and 500 nm, for EVA and RASAS, respectively, using the procedure described in Sarkissian et al. (1995b). An ozonesonde climatology from Tenerife was used for O_3 and temperature profiles. A single set of AMFs has been used for all years since both NO_2 and stratospheric temperature variations throughout the season in subtropical regions are small. No aerosols have been included in the calculations.

Stratospheric annual mean temperatures over Izaña for the same 1993–2005 period have been obtained from the monthly mean assimilation data provided by the British Atmospheric Data Centre calculated using the daily analyses from the United Kingdom Met Office. The original data set includes temperature on the standard UARS pressure levels, from surface to 0.316 hPa, on a 2.5° latitude by 3.75° longitude global grid. The data assimilation system used data from operational meteorological observations.

3.3 Errors

Uncertainties in UV-Vis spectrometry at zenith during twilight come from three sources: observational errors, uncertainty in NO2 cross-sections and AMF calculations. Typical fitting errors range from 1–2% under clear skies and 2–3% in cloudy conditions. The uncertainty in the Vandaele et al. (1998) NO_2 cross-sections is estimated to be 2% or better. These cross-sections are recommended as standard by Orphal (2002) in his comprehensive review. The AMF depends on the shape of the NO_2 profile distribution. The NO_2 profile changes from sunrise to sunset and from winter to summer due to photochemistry. Accurate VCD AMFs require day-to-day calculations based on a realistic NO_2 profiles. For practical reasons a single AMF-set computed for the AFGL tropical profile has been used. Radiative transfer calculations based on the INTA fully spheri-

cal single scattering model for solstices and sunrise and sunset have been performed to estimate the error introduced by this approximation. Profiles have been extracted from the NO_2 harmonic climatology by Lambert et al. (2000) based on HALOE v19 and POAM-III data. AMF differences between this climatology and the AFGL-tropical used as reference for summer-winter and am-pm in the 89°–91° sza range, are of the order of 5%. The overall uncertainty due to AMF is estimated to be 6–7%.

The differential cross-section of NO_2 in the visible range depends on temperature. Retrievals using stratospheric temperatures (i.e. 220 K) yield too low NO_2 when the actual temperature is larger. Figure 2 shows the magnitude of the error as a function of the effective temperature of the atmosphere for the 435–540 nm spectral range based on the Vandaele et al. (1998) cross-section. The effective temperature at a given sza is defined as the mean temperature of the atmosphere weighted by the NO_2 concentration at each layer contributing to the total observed rays:

$$\mathrm{Teff(sza)} = \frac{\int_0^{\mathrm{top}} \mathrm{NO_2}(z) \cdot WF(\mathrm{sza}, z) \cdot T(z) dz}{\int_0^{\mathrm{top}} \mathrm{NO_2}(z) \cdot WF(\mathrm{sza}, z) dz} \quad (7)$$

where *WF(*sza,*z)* are the normalized weighting functions for each altitude. Since the altitude of the maximum scattering is strongly dependent on the sza during twilight a large change in the effective temperature is observed at high sza (Fig. 3). If a unique NO_2 cross-section is used during the day an underestimation of 10 to 13% occurs at noon due to this effect. Except for the investigation of the diurnal variation, only spectra at around sza of 90° have been used in this work. Under these conditions, the effective temperature matches the cross-section temperatures (220 K). A ±3% uncertainty can be attributed to changes in the effective temperature at twilight during the year.

The FOV of the instrument also has an impact in the retrieved columns. The observed spectrum results from the integration of rays of different directions within the FOV, while the column is referred to an ideal pure zenith line. We can define an effec-

tive path, $\overline{R}$, dependent on the semi FOV (α) as:

$$\overline{R} = \frac{\sec\alpha - 1}{\ln(\sec\alpha)} \quad (8)$$

For the FOV's used in our instruments $\overline{R}$ is less than 1% larger than the pure vertical or, in other words, we expect an underestimation of the column of less than 1% due to this effect.

3.4 Homogenization of the dataset

In order to minimise the impact of the switch from scanning instrument to PDA on the data record, both instruments have been kept in parallel operation at Izaña for an extended time period. In Fig. 4a the VCD from the scanning-EVA and the PDA-RASAS are shown for the twilight mean between 89° and 91° for the overlapping years 2000 and 2001. Cross-correlation shows no deviation from unity in the slope (Fig. 4b), the standard deviation being 1.6×10^{14} molec/cm^2. When separating between am and pm data the slope changes slightly to 0.96 and 1.03, respectively. As a consequence of these excellent results, no corrections have been applied to the data subsets.

4 SLIMCAT model

SLIMCAT is an off-line 3-D chemical transport model (CTM) described in detail by Chipperfield (1999) and Chipperfield (2006). The model has been used in many studies of stratospheric chemistry and has been shown to perform well (e.g. Feng et al., 2006). The model contains a gas-phase stratospheric chemistry scheme along with a treatment of heterogeneous chemistry on liquid aerosols and liquid/solid polar stratospheric clouds (PSCs). Horizontal winds and temperatures are specified using meteorological analyses (e.g. from European Centre for Medium-Range Weather Forecasts

(ECMWF)) while vertical transport in the stratosphere is diagnosed from calculated heating rates.

In this study the model was run at a resolution of 7.5°×7.5° with 24 hybrid $\sigma-\theta$ levels from the surface to approximately 60 km. Two runs were performed; the first (run A) was a simulation with free-running chemistry. The model was integrated from 1977 until 2006 using ECMWF analyses (ERA-40 up to 2001, then operational). Chemical boundary conditions were applied by specifying surface mixing ratios of source gases based on past observations (WMO, 2003). In this run the distribution of chemical species is therefore determined by the modelled chemistry and transport. A second model run (run B) was performed which included chemical data assimilation. Run B started in 1991 (initialised from run A) but with assimilation of HALOE O_3, CH_4, H_2O and HCl. The method of chemical data assimilation used in this model is described in Chipperfield et al. (2002) and uses the sequential technique of Khattatov et al. (2000) along with preservation of model-predicted tracer-tracer correlations. In effect, the assimilation of the long-lived tracer CH_4 constrains all of the modelled long-lived tracer and serves to correct errors in the modelled transport (as provided by the forcing analyses).

Model output was saved every 2 days (at 00:00'UT) interpolated to the location of Tenerife. A stacked chemical box model was then run to obtain model output at the correct time of day for comparison with the observations (sunrise and sunset at 90° sza).

5 Results

5.1 Diurnal variations

Although optimized for twilight observations, DOAS visible spectroscopy can be used to study the diurnal evolution of the NO_2. Measurements at low SZA are challenging since they are highly sensitive to instrumental noise, accuracy in air mass factors and atmospheric conditions. Additionally, the impact of the uncertainty in the reference

content to the VCD, which is small at twilight, increases at low SZA since measured SCD approach zero towards noon. A wrong estimation of the absorber content in the reference results in a strong diurnal variation with either too large an increase (excess) or too low (defect of reference content).

For these reasons we have selected days with extremely low aerosol content resulting in very large signal to noise ratio. In Fig. 5 an example is shown for winter solstice. The diurnal variation has been constrained by considering that, once the day conditions are established, NO_2 VCD increases linearly during the day, between 80° morning and evening, essentially due to photodissociation of N_2O_5 (Solomon et al., 1986). A value of 6×10^{15} molec cm^{-2} in the reference content is obtained in this way. Measurements start at sza of 93.3° am and end at 93.6° pm when the sky illumination is too low. Data gaps between 65° and 70° in am and pm are due to the instrument scheduling configuration for off-axis measurements. The result of the integration of the adapted SLIMCAT box model for the same day and latitude is also shown (Denis et al., 2005). A fixed amount of 3×10^{14} molec cm^{-2} is added to the model data to fit the observations. The good agreement in the diurnal behaviour provides an observational evidence of the accuracy of the model NOy chemistry in low latitudes.

5.2 Seasonal variability

The climatological seasonal wave has been obtained as the mean for each day of all the years considered (Fig. 6). Mean annual values are of 2.51×10^{15} and 3.79×10^{15} molec cm^{-2} for am and pm, respectively. Although strongly modulated by photochemistry through the number of light hours in the stratosphere, a spring-autumn asymmetry occurs. The maximum departure from pure photochemical control takes place at 13–13.5 h of light (March–October) (Fig. 7). The asymmetry is due to a secondary wave which is phase-shifted by 3 months with respect to the primary one, having an amplitude of 2.8×10^{14} and 4.5×10^{14} molec cm^{-2} for the am and pm data, respectively. A relative contribution to the VCD of about 6% during the equinoxes (Fig. 8a) results in a shifting of the NO_2 VCD maximum/minimum toward spring/autumn. The

secondary wave has been found to be highly correlated to the temperature in the upper stratosphere. The sign of the correlation is the opposite of that expected from an artefact resulting from temperature changes not treated in the retrieval. Figure 8b displays the correlation between the NO_2 secondary wave contribution to the VCD and the mean temperature from UKMO for the same time period (1993–2006), showing how the observed modulation is dominated by the layer above 5 hPa (~36 km) where the correlation coefficient is over 0.85. The change in NO_2 due to temperature can be estimated for daytime by computing the ratio

$$\frac{NO}{NO_2} \approx \frac{J_{NO2} + k_1[O]}{k_2[O_3]} \quad (9)$$

where k_1 and k_2 are the reaction constants of $NO_2 + O \rightarrow NO + O_2$ and $NO + O_3 \rightarrow NO_2 + O_2$, respectively. This yields an almost linear increase of 1.5%/K assuming constant concentrations of [O] and [O_3], that is 6% for the 4K amplitude of the temperature wave in the upper stratosphere in good agreement with observations.

5.3 Interannual variability

The monthly mean NO_2 data record since 1993 is shown in Fig. 9a. The column displays an increase in the first years due to the recovery from stratosphere partial denoxification after the Mt. Pinatubo eruption in 1991, observed as a general feature in ground based datasets (Johnston et al., 1992; Koike et al., 1993; Van Roozendael et al., 1997; Liley et al. 2000). However, other interannual variability can also be seen from the observational record. From 2002 onwards a decrease in the amplitude of the annual wave is observed. Departures from the seasonal mean (Fig. 9b) can be due to a number of effects such as changes in the meridional component of dominant winds in the mid stratosphere due to drifting in quasi-stationary waves or the QBO, changes in temperature, etc. An interpretation of these features requires a detailed knowledge of the dynamics and chemistry of the region and is out of the scope of this work. Trends are not obvious from the figure and in no case are statistically significant.

5.4 Ground-based versus satellite

Ground-based am NO_2 VCDs have been compared to GOME (ERS-2) and SCIAMACHY (ENVISAT) VCD data retrieved at the University of Bremen (Richter et al., 2005a; Richter et al., 2005b) updated to version 2.0. The satellite data are based on DOAS retrievals performed in the 425–450 nm range with essentially the same settings as used for the ground-based instruments, except for the NO_2 cross-sections. For GOME, the NO_2 cross-sections of (Burrows et al., 1998) at 241 K was used, for SCIAMACHY the Bogumil et al. (2003) values at 243 K. Due to the lack of simultaneity between measurements, the diurnal change of the VCD must be taken into account for a proper intercomparison (Lambert et al., 2004; Sussmann et al., 2005). Following box model results and observations (see Fig. 5), the NO_2 VCD continues decreasing due to photodissociation well after the 90° am DOAS measurements. The column recovers during daytime at a rate of 6×10^{13} molec/cm^2/h and equals the am twilight after noon (fractional day 0.58 and 0.62 in winter and summer, respectively). ENVISAT overpasses the station at around 10:00 Solar Local Time (SLT) or fractional day 0.42, therefore a 2.3 to 2.9×10^{14} molec/cm^2 lower values in SCIAMACHY data would be expected due to this effect. GOME overpass is half an hour later and the difference with the ground-based data should be 3×10^{13} molec/cm^2 less. A fraction of it would be compensated by the smaller NO_2 column observed by the ground-based spectrograph as compared to the satellite due to the height of the observatory. Additional uncertainties result from the different line of sight of both instruments. Maximum sensitivity of ground-based zenith instrumentation at dawn occurs some 200 km in the direction towards sunrise. While this difference must be considered at high latitudes where NO_2 zonal gradients can be significant, its contribution at tropical regions is within the error bars and has not been taken into account in this work.

Figure 10 displays the satellite NO_2 VCD superimposed on the GB-DOAS. One year of overlap between GOME and SCIAMACHY shows consistency in magnitudes between both instruments. When compared to the ground-based data, SCIAMACHY

ACPD
7, 15067–15103, 2007

shows excellent agreement while GOME data produces too low summer values and the annual maximum shifted towards spring. SCIAMACHY minus GB differences are 1.1% on average (Fig. 11a) with a moderate standard deviation of 2.2×10^{14} molec/cm^2. GOME yields lower values (−9.4%) and larger standard deviation 3.0×10^{14} molec/cm^2 (Fig. 11b).

As discussed above, the satellite data should be slightly lower than the ground-based measurements as result of the photochemical change of NO_2 over the day. However, this is not the case for SCIAMACHY but too strongly for GOME. For SCIAMACHY, the most probable reason is the use of a NO_2 cross-section at 243 K instead of 220 K which leads to a systematic overestimation of about 6% (2×10^{14} molec/cm^2 in summer, 1.2×10^{14} molec/cm^2 in winter). For GOME NO_2 columns, a spectral interference pattern induced by the diffuser plate used for irradiance measurements prevents the use of the solar measurements as reference (Richter and Burrows, 2002). Therefore, a normalisation over the Pacific region is used assuming a constant NO_2 column in that region (Richter et al., 2005a) which strongly limits the information content of GOME measurements at low latitudes. The poorer agreement of GOME data compared to SCIAMACHY measurements (which do not suffer from such an effect) is therefore to be expected.

5.5 Ground-based versus SLIMCAT

Figure 12 shows the comparison of observed and modelled sunrise and sunset column NO_2 at Izaña. The chemically free running model (run A) reproduces the general shape of the observed NO_2 VCD seasonal cycle but underestimates the magnitude throughout spring and summer. The maximum underestimation is more marked at sunrise (25%) than at sunset (12%). When chemical data assimilation is included (run B) the model-observation comparison improves considerably. The modelled sunrise NO_2 VCD now agrees very well in magnitude throughout the annual cycle, although the winter minimum in the observations is overestimated (15%). The sunset agreement is also much better although, as with the sunrise plot, there is an overestimation of the

winter minimum seen in the observations (25%). Note that in the assimilation run B the winter minimum is too high.

Clearly, the model run constrained by chemical data assimilation compares better with observations but it is important to bear in mind how that has been achieved and to remember where comparisons are still meaningful. In the case of run B assimilation of HALOE CH_4 constrains this modelled field to mimic the observations. Through preserved tracer-tracer correlations the modelled N_2O field is transformed and then so is NOy. In effect the CH_4 constraint modifies the model NOy to be consistent. These changes to the long-lived tracers are correcting errors in the modelled transport. The partitioning of chemical species within the NOy family is then controlled by the model chemistry, as before, although changes to the model O_3 through assimilation will affect this slightly. Overall we can say that the assimilation run B is therefore still testing the model NOy chemistry but, compared to run A, has been corrected for uncertainties in modelled transport.

Figure 12 indicates, therefore, that chemical assimilation improves upon the transport in the model which is determined by the quality of the winds used to force it. There are known problems with the ability of assimilated winds to represent transport in the sub-tropics; analyses tend to allow too much transport from the tropics to mid-latitudes (e.g. Schoeberl et al. 2003).

Clearly, both model runs capture the seasonal cycle in column NO_2, although run A underestimates the summer maximum due to transport errors. Run B has improved upon run A, in effect having been corrected for these transport errors. However, run B overestimates the winter minimum by 10% at sunrise and 20% at sunset. In run B the modelled NO_2 column generally increases relative to run A because of large NO_2 mixing ratios in the lower stratosphere associated with larger NOy (and smaller N_2O). Without suitable observations (e.g. profiles of NOy and N_2O_5) it is not possible to confirm the accuracy of the other model NOy species and explain the reason for the increase in winter column NO_2.

6 Summary

Fourteen years of daily NO_2 vertical column density (VCD) measurements by zenith sky spectroscopy at the unpolluted NDACC station of Izaña (28° N, 16° W, 2370 m a.s.l.) starting in 1994 have been used for analysing the NO_2 climatology in the northern subtropics from diurnal to interannual timescales. The overall uncertainty in the data are estimated at 10–12% considering measurements errors, cross-sections uncertainties and Air Mass Factors approximations.

NO_2 VCD from continuous measurements between 95° am to 95° pm display a diurnal cycle in good agreement with a vertically integrated gas-phase chemical box model providing observational evidence that the diurnal cycle at low latitudes are dominated by the solar radiation through the NOx partitioning. The seasonal cycle is mainly controlled by the available hours of light, but modulated by the temperature in the upper stratosphere. This secondary annual wave contributes 6% to the total column and is phase-shifted by 3 months (maximum in spring) with respect the astronomical wave resulting in a shifting of the NO_2 VCD maximum toward spring and a flatness of the summer maximum and winter minimum. Mean values are of 2.51×10^{15} and 3.79×10^{15} molec cm^{-2} for am and pm, respectively. Interannual variability of up to 10% in the annual maxima is observed from the monthly mean record but from the available dataset no trend can be inferred.

Ground-based data have been compared with the GOME (ERS2) and SCIAMACHY (ENVISAT) orbital spectrometers in nadir looking mode processed by the University of Bremen v2.0. SCIAMACHY NO_2 VCD yield an excellent agreement with ground-based data while GOME displays too low values in summer due to a spectral interference pattern induced by the diffuser plate. Mean differences between GB minus satellite are of +1.1% for SCIAMACHY and −9.6% for GOME.

Additionally, a comparison between data and modelling have been carried out using the long-term output of the SLIMCAT 3-D CTM. The basic model run A, forced by ECMWF (ERA-40) analyses, captures the observed NO_2 annual cycle but significantly

underestimates the spring/summer maximum. A second model run B, which assimilated HALOE profiles of CH_4 to constrain the model long-lived tracers, showed much better agreement. This improvement in modelled column NO_2 is likely due to better modelled NOy profiles and points to transport errors in the ECMWF ERA-40 reanalyses. The impact of this on CTM studies of long-term trends in NO_2 and O_3 needs further investigation.

Acknowledgements. The authors want to acknowledge the Izaña operational team and C. López for the instrument maintenance. C. Fayt and M. Van Roozendael (BIRA/IASB) kindly provided the WINDOAS package for cross-sections convolution to the field instruments. J. C. Lambert (BIRA/IASB) provided the NO_2 climatology based on satellite used in the SLIMCAT box model adapted by L. Denis and H. Roscoe (BAS). Upper temperature data were collected from the British Atmospheric Data Centre. Routine measurements have been possible thanks to the funding provided by the projects QUILT (EU EVK2-CT2000-0059) SCOUT-O3 (EU 505390-GOCE-CT-2004), TROMPETA (MCyT CGL2004-03669) and is on-going through GEOMON (EU FP6-2005-Global-4-036677).

References

Bogumil, K., Orphal, J., Flaud, J.-M., and Burrows, J.-P.: Vibrational Progressions in the Visible and Near Ultraviolet Absorption Spectrum of Ozone, Chem. Phys. Lett., 349, 241–248, 2001.

Bogumil, K., Orphal, J., Homann, T., Voigt, S., Spietz, P., Fleischmann, O. C., Vogel, A., Hartmann, M., Bovensmann, H., Frerick, J., and Burrows, J. P.: Measurements of molecular absorption spectra with the SCIAMACHY Pre-Flight Model: instrument characterization and reference data for atmospheric remote-sensing in the 230–2380 nm region, J. Photoch. Photobio. A, 157, 167–184, 2003.

Brewer, A. W., McElroy, C. T., and Kerr, J. B.: Nitrogen dioxide concentration in the atmosphere, Nature, 246, 129–133, 1973.

Burrows, J. P., Dehn, A., Deters, B., Himmelmann, S., Richter, A., Voigt, S., and Orphal, J.: Atmospheric remote-sensing reference data from GOME: Part 1. Temperature-dependent absorption cross-sections of NO_2 in the 231–794 nm range, J. Quant. Spectrosc. Ra., 60, 1025–1031, 1998.

Chipperfield, M. P.: Multiannual simulations with a three-dimensional chemical transport model, J. Geophys. Res., 104, 1781–1805, 1999.
Chipperfield, M. P., Khattatov, B. V., and Lary, D. J.: Sequential assimilation of stratospheric chemical observations in a three-dimensional model, J. Geophys. Res., 107, 4585, doi:10.1029/2002JD002110, 2002.
Chipperfield, M. P.: New Version of the TOMCAT/SLIMCAT Off-Line Chemical Transport Model: Intercomparison of Stratospheric Tracer Experiments, Q. J. Roy Meteor. Soc., 132, 1179–1203, doi:10.1256/qj.05.51, 2006.
Denis, L., Roscoe, H. K., Chipperfield, M. P., Van Roozendael, M., and Goutail, F.: A new software suite for NO_2 vertical profile retrieval from ground-based zenith-sky spectrometers, J. Quant. Spectrosc. Ra., 92(3), 321–333, 2005.
Fayt, C. and Van Roozendael, M.: WinDOAS 2.1. User Manual, IASB-BIRA, 2001.
Feng, W., Chipperfield, M. P., Dorf, M., Pfeilsticker, K., and Ricaud, P.: Mid-latitude Ozone Changes: Studies with a 3-D CTM Forced by ERA-40 Analyses, Atmos. Chem. Phys., 7, 2357–2369, 2007, http://www.atmos-chem-phys.net/7/2357/2007/.
Greenblatt, G. D., Orlando, J. J., Burkholder, J. B., and Ravishankara, A. R.: Absorption Measurements of Oxygen Between 330 and 1140 nm, J. Geophys. Res., 95, 18 577–18 581, 1990.
Hendrick, F., Van Roozendael, M., Lambert, J.-C., and de Mazière, M.: Validation of MIPAS NO_2 profiles and columns using ground-based zenith-sky UV-visible observations. Geophysical Research Abstracts, 6, 10-2-2004. EGU 2004.
Johnston, P. V., McKenzie, R. L., Keys, J. G., and Matthews, W. A.: Observations of depleted stratospheric NO_2 following the Pinatubo volcanic eruption, Geophys. Res. Lett., 19, 211–213, 1992.
Khattatov, B. V., Lamarque, J. F., Lvjak, L. V., Menard, R., Levelt, P., Tie, X. X., Brasseur, G. P., and Gille, J. C.: Assimilation of satellite observations of long-lived chemical species in global chemistry transport models, J. Geophys. Res., 105, 29 135–29 144, 2000.
Koike, M., Kondo, Y., Matthews, W. A., Johnston, P. V., and Yamazaki, K.: Decrease of stratospheric NO_2 at 44° N caused by Pinatubo Volcanic aerosols, Geophys. Res. Lett., 20, 1975–1978, 1993.
Lambert, J.-C., Van Roozendael, M., Simon, P. C., De Mazière, M., Pommereau, J.-P., Goutail, F., and Sarkissian, A.: Pole-to-pole validation of GOME level-2 products with ground-based

networks, Earth Observation Quarterly, 58, 1998.
Lambert, J.-C., Granville, J., Van Roozendael, M., Müller, J.-F., Goutail, F., Pommereau, J.-P., Sarkissian, A., Johnston, P. V., and Russell III, J. M.: Global Behavior of Atmospheric NO_2 as Derived from the Integrated Use of Satellite, Ground-based Network and Balloon Observations, Atmospheric Ozone. XIX Quadrennial Ozone Symposium, Sapporo, Hokkaido, Japan, 3–8 July 2000.
Lambert, J.-C., Blumenstock, T., Boersma, F., Bracher, A., De Maziere, M., Demoulin, P., De Smedt, I., Eskes, H., Gil, M., Goutail, Granville, J., F., Hendrick, F., Ionov, D. V., Johnston, P. V., Kostadinov, I., Kreher, K., Kyrö, E., Martin, R., Meier, A., Navarro-Comas, M., Petritoli, A., Pommereau, J.-P., Richter, A., Roscoe, H. K., Sioris, C., Sussmann, R., Van Roozendael, M., Wagner, T., Wood, S., and Yela, M.: Geophysical validation of SCIAMACHY NO2 vertical columns: overview of early 2004 results, Proc. of the Second Workshop on the Atmospheric Chemistry Validation of ENVISAT (ACVE-2), ESA ESRIN, Frascati, Italy, 3–7 May 2004, ESA SP-562, 2004.
Lambert, J.-C., Granville, J., Hendrick, F., Andersen, S. B., Dorokhov, V., Gerard, P., Gil, M., Goutail, F., Gruzdev, A. N., Held, G., Ionov, D. V., Johnston, P. V., Kostadinov, I., Kreher, K., Kyro, E., Lerot, C., Leveau, J., Navarro-Comas, M., Petritoli, A., Pommereau, J.-P., Richter, A., Roscoe, H. K., Semenov, V. K., Stebel, K., Van Roozendael, M., Vaughan, G., Wagner, T., Wittrock, F., and Yela, M.: Transfer of GOME Data Processor (GDP) version 4.0 to SCIAMACHY Off-line (OL) processor version 3.0: Pole-to-pole delta-validation of NO_2 column data with the NDACC/UV-Visible network, Procc. Of the Third Workshop on the Atmospheric Chemistry Validation of Envisat (ACVE-3), ESA SP-642, 2007.
Lee, A. M., Roscoe, H. K., Oldham, D. J., Squires, J. A. C., Sarkissian A., and Pommereau, J.-.P.: Improvements to the accuracy of measurements of NO_2 by zenith-sky visible spectrometers, J. Quant. Spectrosc. Ra., 52, 5, 649-657, 1994.
Liley, J. B., Johnston, P. V., McKenzie, R. L., Thomas, A. J., and Boyd, I. S.: Stratospheric NO_2 variations from a long time series at Lauder, New Zealand, J. Geophys. Res., 105(D9), 11 633–11 640, 10.1029/1999JD901157, 2000.
Medeke, T., Fietkau, S., Oetjen, H., Richter, A., Wittrock, F., and Burrows, J. P.: SCIAMACHY validation with the BREDOM network, Geophysical Research Abstracts, 7, 05159, 2005.
Minschwaner, K., Salawitch, R., and McElroy, M.: Absorption of solar radiation by O_2: Implications for O_3 and lifetimes of N_2O, $CFCl_3$ and CF_2Cl_2, J. Geophys. Res., 98, 10 543–10 561, 1993.

NDACC web page: http://www.ndsc.ncep.noaa.gov/, 2007.
Noxon, J. F.: Nitrogen Dioxide in the stratosphere and troposphere measured by ground-based absorption spectroscopy, Science, 189, 547–549, 1975.
Orphal, J. A.: Critical Review of the Absorption Cross-Sections of O3 and NO2 in the 240–790 nm Region, Part 2. Nitrogen Dioxide, ESA Technical Note MO-TN-ESA-GO-0302, 2002.
Piters, A. J. M., Bramstedt, K., Lambert, J.-C., and Kirchhoff, B.: Overview of SCIAMACHY validation: 2002–2004, Atmos. Chem. Phys., 6, 127–148, 2006, http://www.atmos-chem-phys.net/6/127/2006/.
Richter, A. and Burrows, J. P.: Retrieval of Tropospheric NO_2 from GOME Measurements, Adv. Space Res., 29(11), 1673–1683, 2002.
Richter, A., Wittrock, F., Weber, M., Beirle, S., Kühl, S., Platt, U., Wagner, T., Wilms-Grabe, W., and Burrows, J. P.: GOME observations of stratospheric trace gas distributions during the splitting vortex event in the Antarctic winter 2002 Part I: Measurements, J. Atmos. Sci., 62(3), 778–785, 2005a.
Richter, A., Burrows, J. P., Nüß, H., Granier, C., and Niemeier, U., Increase in tropospheric nitrogen dioxide over China observed from space, Nature, 437, 129–132, doi:10.1038/nature04092, 2005b.
Richter, A., Kreher, K., Johnston, P. V., Wittrock, F., and Burrows, J. P.: Validation of GOME O_3, NO_2, BrO, and OClO Measurements in Southern High Latitudes, Procc. of the Fifth European Workshop on Stratospheric Ozone, European Commission, Air Pollution research report, 73, 719–722, 2000.
Richter, A., Burrows, J. P., Fietkau, S., Medeke, T., Notholt, J., Oetjen, H., Sierk, B., Warneke, T., Wittrock, F., Dix, B., Friess, U., Wagner, T., Blumenstock, T., Griesfeller, A., Sussmann, R., Rockmann, A., and Schultz, A.: A Scientific NO_2 product from Sciamachy: First Results and validation. Proc. of the Second Workshop on the Atmospheric Chemistry Validation of ENVISAT (ACVE-2), ESA ESRIN, Frascati, Italy, 3–7 May 2004, ESA SP-562, 2004.
Rinsland, C. P., Weisenstein, D.K., Ko, M. K. W., Scott, C. J., Chiou, L. S., Mahieu, E., Zander, R., and Demoulin, P.: Post-Mount Pinatubo eruption ground-based infrared stratospheric column measurements of HNO_3, NO, and NO_2 and their comparison with model calculations, J. Geophys. Res., 108(D15), 4437, doi:10.1029/2002JD002965, 2003.
Roscoe, H.K., Johnston, P.V., Van Roozendael, M., Richter, A., Sarkissian, A., Roscoe, J., Preston, K.E., Lambert, J.C., Hermans, C., Decuyper, W., Dzienus, S., Winterrath, T., Burrows, J., Goutail, F., Pommereau, J.P., D'Almeida, E., Hottier, J., Coureul, C., Didier, R., Pundt, I.,

Bartlett, L. M., McElroy, C. T., Kerr, J. E., Elokhov, A., Giovanelli, G., Ravegnani, F., Premuda, M., Kostadinov, I., Erle, F., Wagner, T., Pfeilsticker, K., Kenntner, M., Marquard, L. C., Gil, M., Puentedura, O., Yela, M., Arlander, D. W., Kastad Hoiskar, B. A., Tellefsen, C. W., Karlsen Tornqvist, K., Heese, B., Jones, R. L., Aliwell, S. R., and Freshwater, R. A.: Slant column measurements of O3 and NO2 during the NDSC intercomparison of zenith-sky UV-visible spectrometers in june 1996, J. Atmos. Chem., 32, 281–314, 1999.

SAOZ web page. http://www.aero.jussieu.fr/themes/CA/Reseau%20SAOZ.html, 2007.

Sarkissian A., Fish, D., Van Roozendael, M., Gil, M., Chen, H. B., Wang, P., Pommereau, J. P., and Lenoble, J.: Ozone and NO_2 air-mass factors for zenith-sky spectrometers: Intercomparison of calculations with different radiative transfer models, Geophys. Res. Lett., 22, 1113–1116, 1995a.

Sarkissian A., Roscoe, H. K., and Fish, D.: Ozone measurements by zenith-sky spectrometers: an evaluation of errors in air-mass factors calculated by radiative transfer models, J. Quant. Spectrosc. Ra., 54, 471–480, 1995b.

Schneider M., Blumenstock, T., Chipperfield, M. P., Hase, F., Kouker, W., Reddmann, T., Ruhnke, R., Cuevas, E., and Fischer, H.: Subtropical trace gas profiles determined by ground-based FTIR spectroscopy at Izaña (28° N, 16° W): Five-year record, error analysis, and comparison with 3-D CTMs, Atmos. Chem., Phys., 5, 153–167, 2005.

Solomon, S., Schmeltekopft, A. L., and Sanders, R. W.: On the interpretation of zenith sky absorption measurements, J. Geophys. Res., 92(D7), 8311–8319, 1987.

Solomon, S., Russell III, J. M., and Gordley, L. L.: Observations of the diurnal variation of Nitrogen dioxide in the stratosphere, J. Geophys. Res., 91(D5), 5455–5464, 1986.

Struthers, H., Kreher, K., Austin, J., Schonfield, R., Bodecker, G., Johnston, P., Shiona, H., and Thomas, A.: Past and future suimulations of NO2 from a coupled chemistry-climate model in comparison with observations, Atmos. Chem. Phys., 4, 2227–2239, 2004, http://www.atmos-chem-phys.net/4/2227/2004/.

Sussmann, R., Stremme, W., Burrows, J. P., Richter, A., Seiler, W., and Rettinger, M.: Stratospheric and tropospheric NO2 variability on the diurnal and annual scale: a combined retrieval from ENVISAT/SCIAMACHY and solar FTIR at the Permanent Ground-Truthing Facility Zugspitze/Garmisch, Atmos. Chem. Phys., 5, 2657–2677, 2005, http://www.atmos-chem-phys.net/5/2657/2005/.

Van Roozendael, M., De Mazière, M., Hermans, C., Simon, P. C., Pommereau, J.-P., Goutail, F., Tie, X. X., Brasseur, G., and Granier, C.: Ground-Based observations of stratospheric NO2

at high and mid-latitudes in Europe after the Mount Pinatubo eruption, J. Geophys Res., 102(D15), 19 171–19 176, 1997.

Vandaele, A. C., Hermans, C., Simon, P .C., Carleer, M., Colins, R., Fally, S., Mérienne, M. F., Jenouvrier, A., and Coquart, B.: Measurements of the NO_2 absorption cross-sections from 42 000 cm^{-1} to 10 000 cm^{-1} (238–1000 nm) at 220 K and 294 K, J. Quant. Spectrosc. Radiat. Transfer, 59, 171–184, 1998.

Vandaele, A. C., Fayt, C., Hendrick, F., Hermans, C., Humbled, F., Van Roozendael, M., Gil, M., Navarro, M., Puentedura, O., Yela, M., Braathen, G., Stebel, K., Tørnkvist, K., Johnston, P., Kreher, K., Goutail, F., Mieville, A., Pommereau, J.-P., Khaikine, S., Richter, A., Oetjen, H., Wittrock, F., Bugarski, S., Friess, U., Pfeilsticker, K., Sinreich, R., Wagner, T., Corlett, G., and Leigh, R.: An intercomparison campaign of ground-based UV-Visible measurements of NO_2, BrO, and OClO slant columns. I. NO_2, J. Geophys. Res., 110(D8), D08305, doi:10.1029/2004JD005423, 2005.

Wetzel, G., Bracher, A., Funke, B., Goutail, F., Hendrick, F., Lambert, J.-C., Mikuteit, S., Piccolo, C., Pirre, M., Bazureau, A., Belotti, C., Blumenstock, T., De Mazière, M., Fischer, H., Huret, N., Ionov, D., Lopez-Puertas, M., Maucher, G., Oelhaf, H., Pommereau, J.-P., Ruhnke, R., Sinnhuber, M., Stiller, G., Van Roozendael, M., and Zhang, G.: Validation of MIPAS- ENVISAT NO_2 operational data, Atmos. Chem. Phys. Discuss., 7, 3333–3395, 2007, http://www.atmos-chem-phys-discuss.net/7/3333/2007/.

WMO, (World Meteorological Organization), Scientific Assessment of Ozone Depletion, 2002, Global Ozone Research and Monitoring Project, Report No 47, 2003.

WMO (World Meteorological Organization). Scientific Assessment of Ozone Depletion: 2006, Global Ozone Research and Monitoring Project, Report No 50, 2007.

Yela, M., Gil, M., Navarro, M., Rodriguez, S., Cuevas E., and Romero, C.: Meridional transport in the subtropics during winter as seen by NO_2 column record, Air Pollution Report 66, EUR 18032EN, edited by: Harris, N. R. P., Kilbane-Dawe, I., and Amanatidis, G. T., 88–91, 1998.

Yela., M., Gil, M., Rodríguez, S., Araujo, J., Ochoa, H., Díaz, S., and Deferrari, G.: Unusual behavior of stratospheric NO_2 during splitting vortex event in the Antarctic winter 2002: Comparison with a 10-years NO_2 climatology at three Antarctic and sub Antarctic sites, Proc. Quadrennial Ozone Symposium, 454, 1–8 June 2004, Kos, Greece.

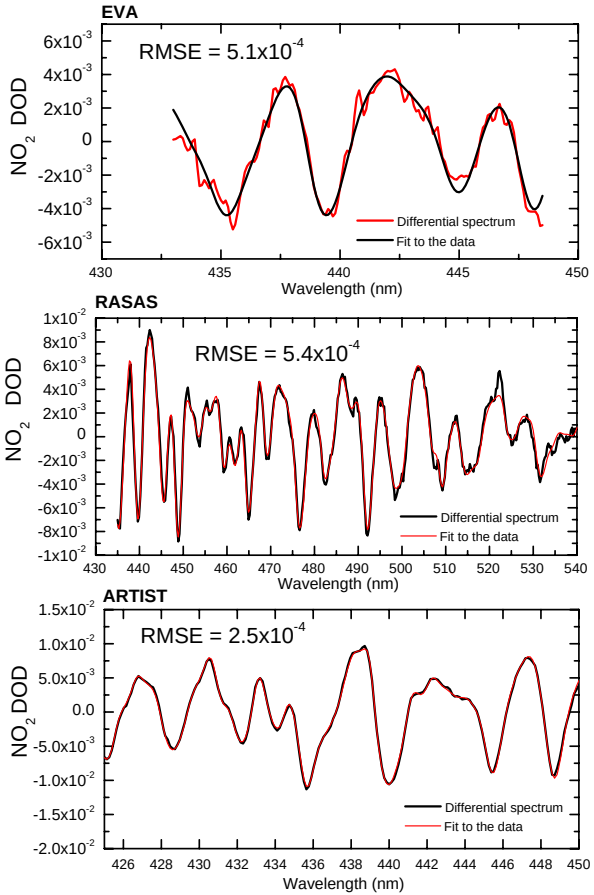

Fig. 1. Examples of spectral fits for the EVA, RASAS and ARTIST ground-based spectrometers for the standard NO_2 retrieval ranges. No smoothing has been applied to the spectra.

ACPD
7, 15067–15103, 2007

EGU

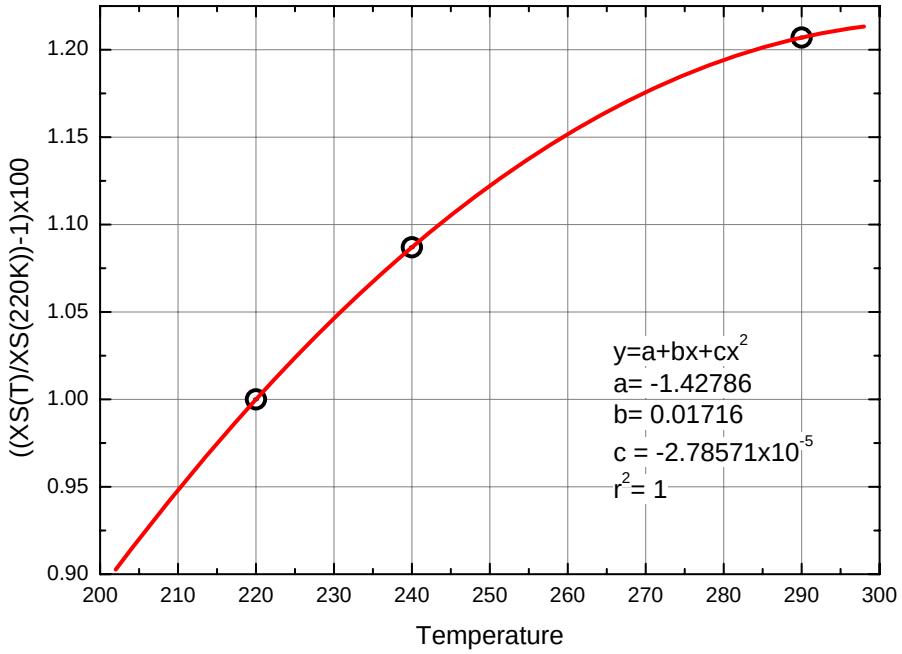

Fig. 2. Magnitude in percent of the errors in the RASAS spectral range if temperatures are different from 220 K, based on Vandaele et al. (1998) cross sections.

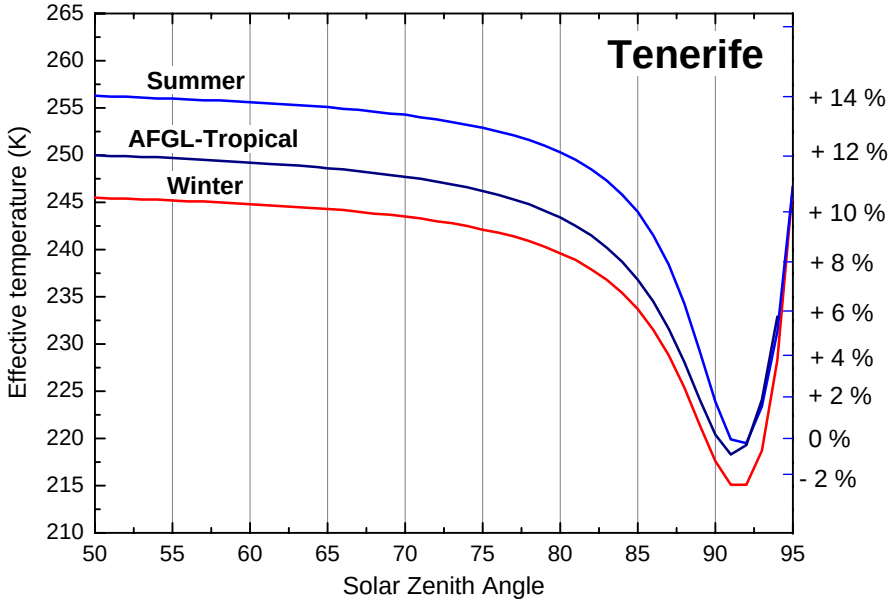

Fig. 3. Effective temperatures above Izaña for the solstices from a radiosonde climatology and the AFGL tropical model.

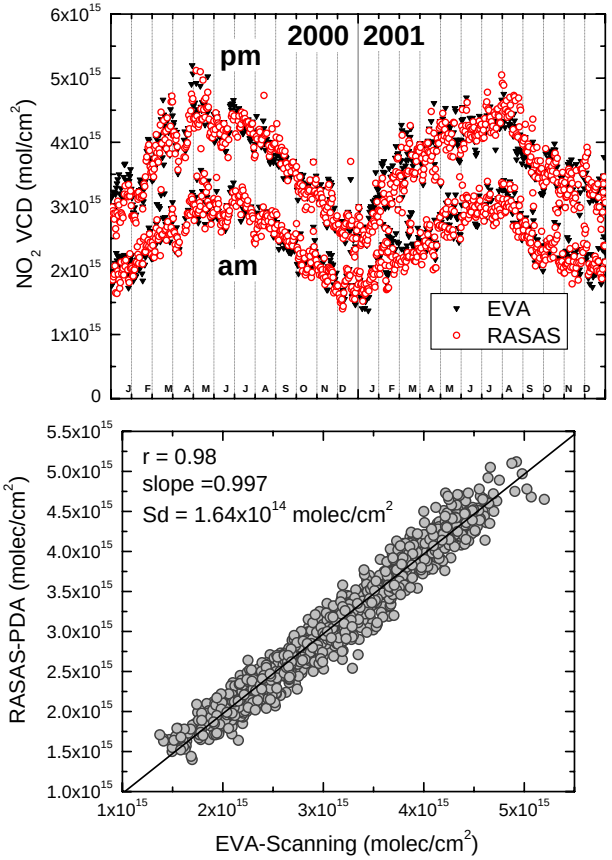

Fig. 4. EVA and RASAS NO_2 VCD for the years 2000–2001 **(a)** and cross-correlation **(b)**.

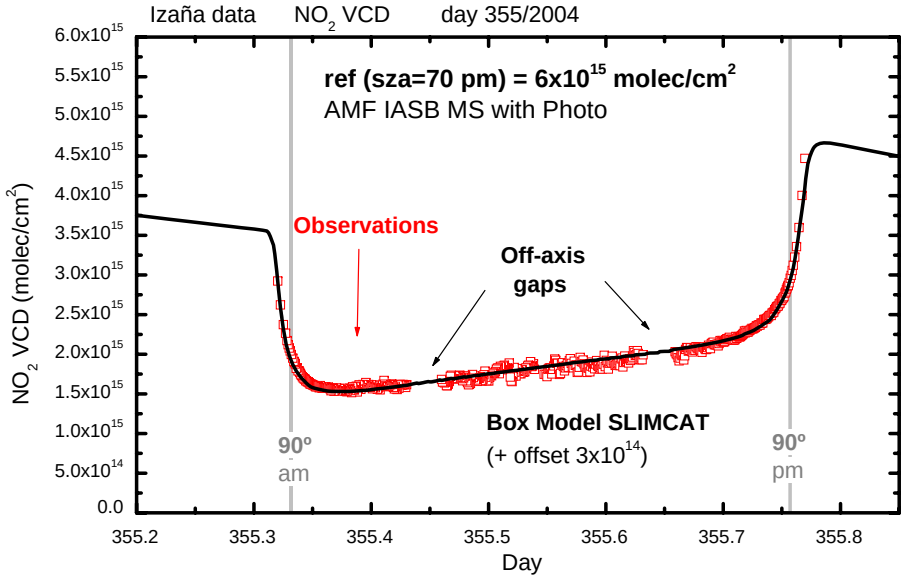

Fig. 5. NO_2 VCD during a day (red squares) versus output from the SLIMCAT photochemical box model.

ACPD
7, 15067–15103, 2007

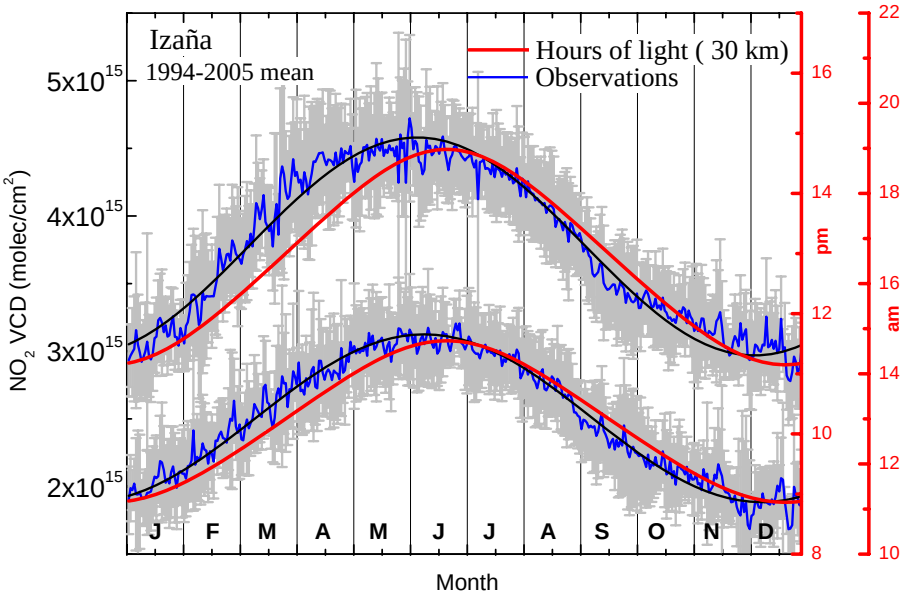

Fig. 6. Climatological seasonal waves for am and pm data (blue lines). Gray error bars represent one standard deviation. The red curves show hours of available sunlight at 30 km on two different scales to show departures from pure photochemical equilibrium. Black lines are the resultant of the fit of primary and secondary waves (see text).

ACPD
7, 15067–15103, 2007

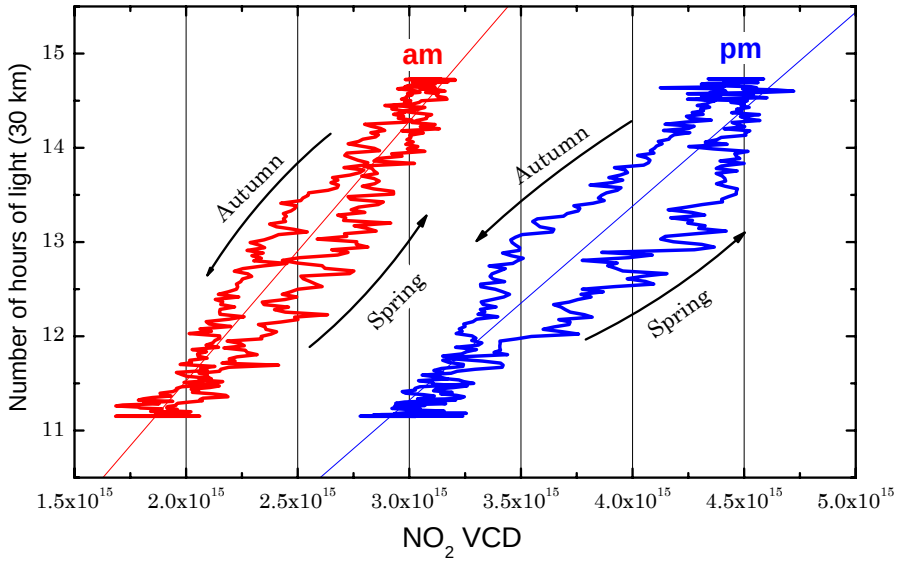

Fig. 7. The NO_2 VCD versus hours of available sunlight at 30 km showing a spring-autumn asymmetry.

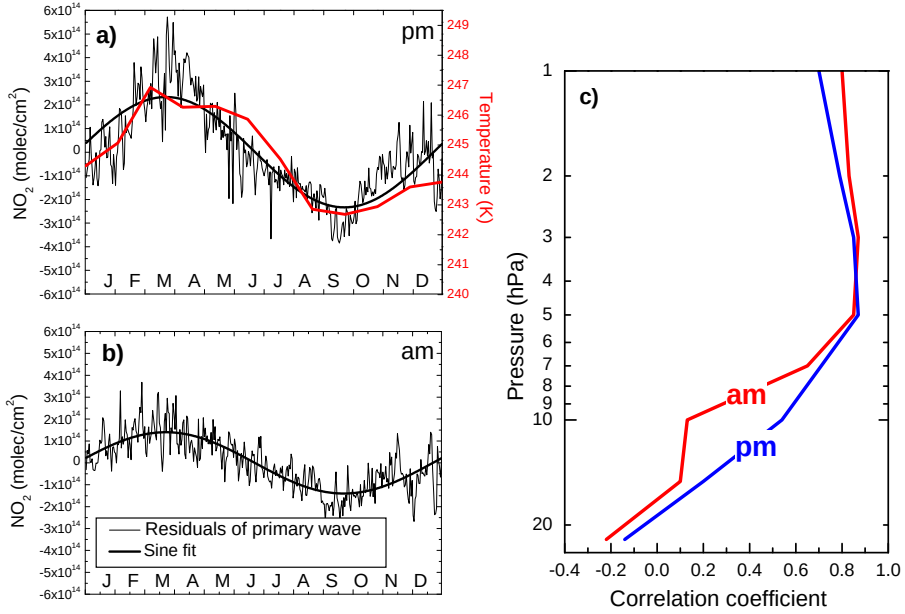

Fig. 8. (a) Amplitude of the secondary wave and temperature at 5 hPa (~36 km). **(b)** Correlation between secondary waves and upper stratosphere temperature.

ACPD
7, 15067–15103, 2007

EGU

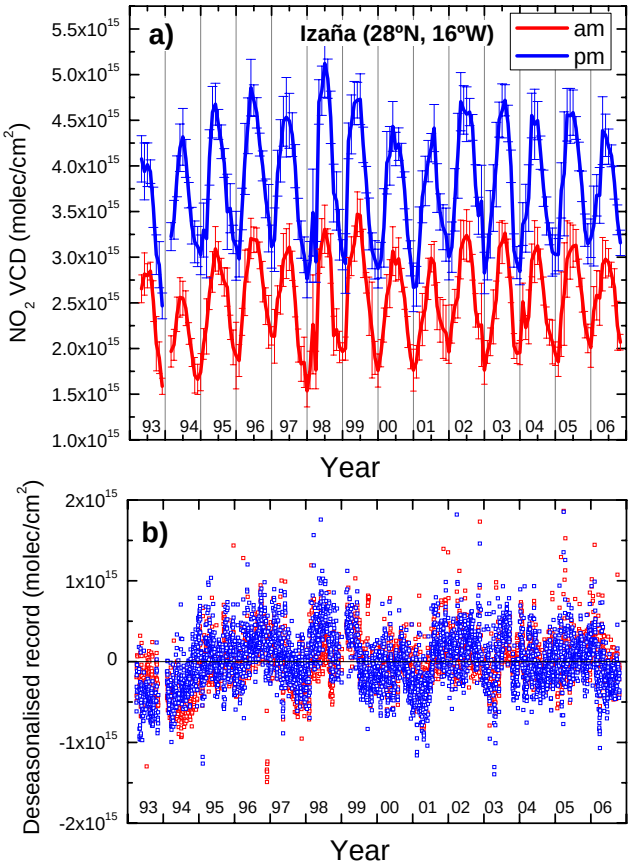

Fig. 9. **(a)** NO_2 monthly mean VCD for am and pm observations from 1993–2006. Error bars represent one standard deviation. **(b)** Deseasonalised departure from monthly mean for am and pm data.

ACPD
7, 15067–15103, 2007

EGU

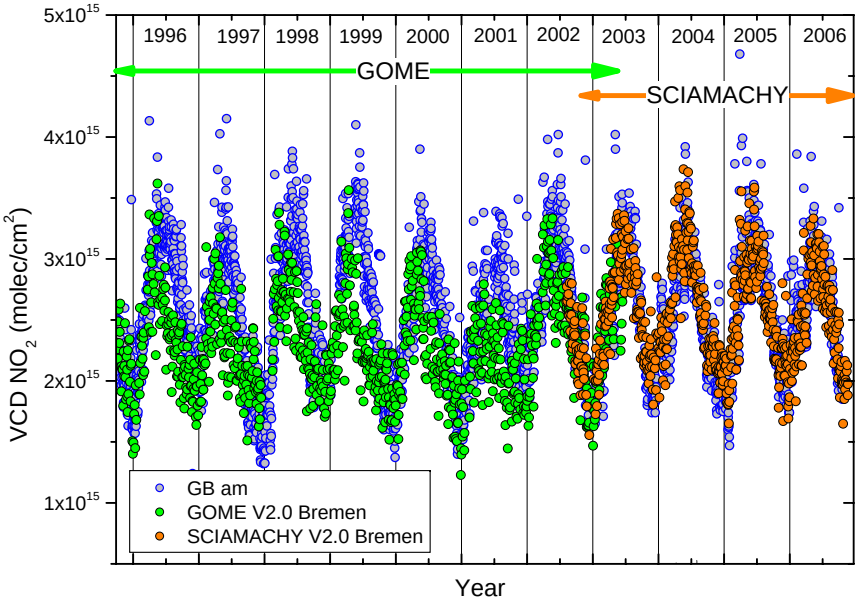

Fig. 10. GOME and SCIAMACHY NO_2 VCD from Bremen v2.0 analysis superimposed on ground based data.

ACPD
7, 15067–15103, 2007

EGU

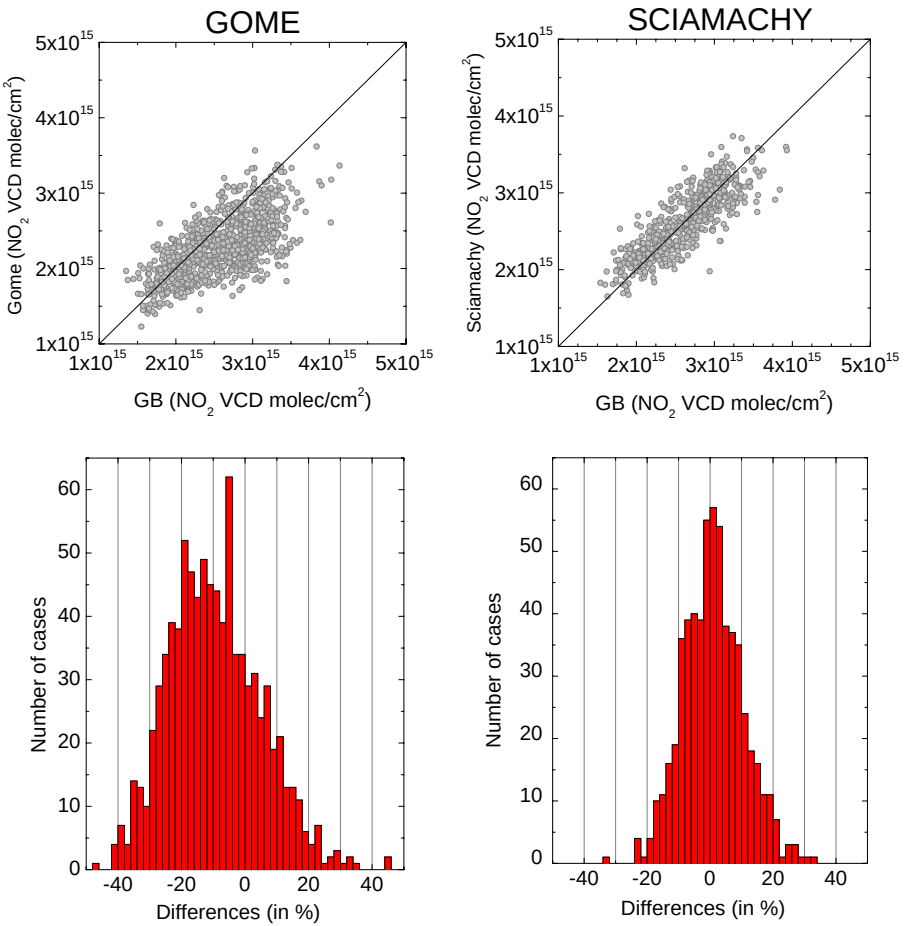

Fig. 11. Satellite – Ground based data cross-correlation (upper panels) and frequency distributions of the differences (lower panels).

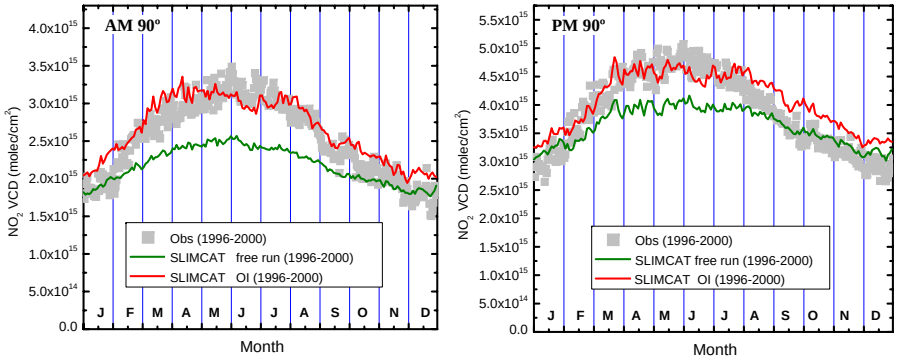

Fig. 12. Mean annual cycle of NO_2 VCD at Izaña (1996–2000) for **(a)** am and **(b)** pm compared with SLIMCAT 3D CTM runs A (green) and B (red).